

## Magnus effect and dynamics of a spinning disc in a rarefied medium

G. MISHURIS<sup>1,2)</sup>, A. PLAKHOV<sup>1,3)</sup>

<sup>1)</sup> *Wales Institute of Mathematical and Computational Sciences  
Institute of Mathematics and Physics, Aberystwyth University, UK*

<sup>2)</sup> *Department of Mechanical Engineering and Aeronautics  
Rzeszów University of Technology, Rzeszów, Poland  
e-mail: miszuris@prz.edu.pl*

<sup>3)</sup> *Department of Mathematics, University of Aveiro, Portugal*

MAGNUS EFFECT consists in deflection of the trajectory of a rotating body moving in a gas. It is a direct consequence of the interaction between the body surface and the gas particles. In this paper, we study the so-called *inverse* Magnus effect which can be observed in rarefied gases. We restrict ourselves to the two-dimensional case, namely a spinning disc moving through a sparse zero-temperature medium. We consider general non-elastic interaction between the disc and the particles depending on the incidence angle. We give a classification of auxiliary parameters with respect to possible dynamical response. In the absence of other forces, three kinds of trajectories are possible: (i) a converging spiral, (ii) a curve converging to a straight line and (iii) a circumference, the case intermediate between the two first ones. A specific 2-D parameter space has been introduced to provide respective classification.

**Key words:** inverse Magnus effect, free molecular flow, non-elastic interaction.

**Mathematics subject classification:** 74F10, 70F40.

Copyright © 2009 by IPPT PAN

### 1. Introduction

LET US CONSIDER A SPINNING BODY moving through a gas. Assuming that the rotation axis is not parallel to the direction of the motion, the created drag force is not parallel to the instant velocity and therefore tends to deflect the body trajectory. This phenomenon is called *Magnus effect* and has been extensively discussed in the literature. Its origin goes back to NEWTON [14] and ROBINS [20] in relation with the dynamics of tennis and cannon balls; see [24] for a historical account. The classical Magnus effect, discussed for a sphere or a cylinder with the symmetry axis orthogonal to its velocity, is a consequence of the transverse force acting on the body whose direction coincides with the instant rotation velocity of the body's front point. Further development of the subject has been maintained during the 20th century due to the interest in sports and technological (mainly military) applications [16, 8, 21, 3, 11, 26].

Recent development in the area related to Magnus effect, alongside with the continuing interest from the modern sport industry and related applications [7, 6, 12], bursts out from the enormous progress in space exploration. A crucial part of the related projects consists of the investigation of satellite aerodynamics in sparse atmosphere. In particular, the following important question should be addressed: how the drag force affects the dynamics of artificial satellites on low Earth orbit and the trajectories of planned space missions to other planets. Moreover, one can ask to what extent the trajectories can be controlled by varying their aerodynamical characteristics [13, 1, 2, 18, 19, 4]. Among other phenomena, a considerable amount of attention has been attracted to the Magnus effect in rarefied gas [5, 9, 25, 27, 23]. In these papers, the gas is supposed to be rarefied to that extent that mutual interaction of molecules can be neglected and therefore, the method of *free molecular flow* [10, 22] is applicable. The bodies have been supposed to be convex and symmetric with respect to the rotation axis (usually a sphere or a cylinder; however, in [9] the general class of bodies was considered). The interaction of the gas particles with the body is considered to be non-elastic; a portion of the tangential component of the particles' momentum is transmitted to the body and, as a result, the transverse force is created. The following conclusion has been made: in extremely rarefied gases the so-called *inverse* Magnus effect takes place. That is, the transverse force acts *opposite* to the rotation velocity of the body's front point. Assuming that the rotation axis is perpendicular to the velocity of translational motion, the formula for the transverse force has been derived (sometimes under additional thermodynamical assumptions [5]):

$$(1.1) \quad F_T = \frac{1}{2} \alpha m v \omega,$$

where  $\alpha$  is the so-called *Maxwellian accommodation coefficient*. Here  $m$  is the mass of the gas displaced by the body,  $\alpha$  is a measure of 'tangential friction' varying between 0 and 1,  $v$  is the velocity of translational motion and  $\omega$  is the angular velocity of the body. It is important to underline that only one parameter friction regime had been analysed thus far resulting in a fixed value of the parameter  $\alpha$ . Note also that the moment of the force has been additionally evaluated in [9, 23].

In [15], as opposed to the papers cited above, the particles are assumed to interact with a *non-convex* body but in the *perfectly elastic* way. The body is a rough disc rotating in the two-dimensional space around the fixed centre. The transverse force here is created due to multiple reflections of particles from small dimples on the disc boundary. The *inverse* Magnus effect is shown to be predominant, and the drag force and the moment of the force have been calculated as functions of the shape of dimples.

By contrast in this paper, addressing the aforementioned question on controllability of the satellite trajectory, we extend the analysis to a general class of non-elastic regimes determined by friction coefficients  $k_1(\varphi)$  and  $k_2(\varphi)$  which may depend on the incidence angle  $\varphi$ . Following WEIDMAN and HERCZYNSKI [27], we assume that the thermal motion of gas particles can be neglected as compared with the velocity of translational motion of the body. We restrict our analysis to the case of a spinning disc translating through two-dimensional space. The main result is that, depending on the friction regime and the inertial properties of the disc, three possible tendencies of its motion can be identified: the trajectory curvature remains constant (I), increases (II) or decreases (III) during the motion. The case (I) is intermediate and separates the cases (II) and (III) determined by two open domains in the parameter space. Stability of the trajectory type with respect to small perturbation of the frictional parameters follows immediately from these results.

The paper is organised as follows. Section 2 contains the main results while Sec. 3 is devoted to numerical examples and discussions.

## 2. Equations of motion

Let us consider a spinning disc moving through a rarefied medium. The latter means that mutual interaction of the particles can be neglected. Additionally, the medium temperature is assumed to be absolute zero; that is, all the particles are initially at rest [27]. The particles collide with the disc according to a non-elastic law to be described below. We choose a local reference system  $\tilde{O}\tilde{x}_1\tilde{x}_2$  connected with the disc boundary in the standard way that the axes  $\tilde{O}\tilde{x}_1$  and  $\tilde{O}\tilde{x}_2$  are, respectively, tangent and normal to the boundary and  $\tilde{x}_2 > 0$  outside the disc (see Fig. 1).

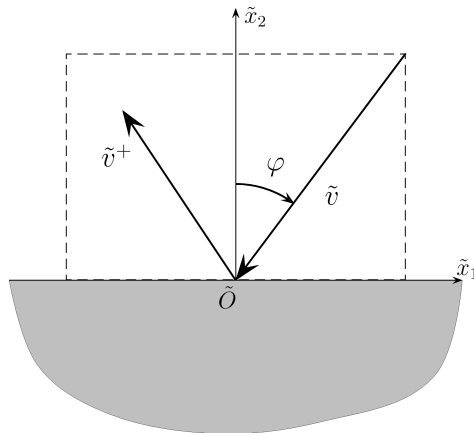


FIG. 1. Non-elastic collision.

In this system the velocity of a particle before collision is  $\tilde{v} = (\tilde{v}_1; \tilde{v}_2)^T$ ,  $\tilde{v}_2 \leq 0$  and

$$(2.1) \quad \tilde{v}^+ = (k_1\tilde{v}_1; -k_2\tilde{v}_2)^T$$

after collision, where  $k_1 = k_1(\varphi)$  and  $k_2 = k_2(\varphi)$  ( $0 \leq k_j \leq 1$ ) can be interpreted as generalised friction coefficients. Here  $\varphi \in [-\pi/2, \pi/2]$  is the angle formed by the velocity of the incident particle and the normal to the disc boundary at the point of collision, measured counterclockwise from the normal. It is natural to assume that  $k_j(\varphi) = k_j(-\varphi)$ .

The reflection law in the coordinate-free form states:  $\tilde{v}^+ = k_1(\tilde{v} - \langle \tilde{v}, n \rangle n) - k_2 \langle \tilde{v}, n \rangle n = k_1\tilde{v} - (k_1 + k_2)\langle \tilde{v}, n \rangle n$ . Here  $\langle \cdot, \cdot \rangle$  means the scalar product, and  $n$  is the outer normal to the body surface.

REMARK 1. As usual (see [5–27]) we assume here and in what follows that the interaction time  $\Delta t$  is infinitesimal in such a sense that at every particular moment  $t_0$  the moving reference system related with the body (the disc) can be considered as inertial one during the time interval  $\Delta t$ .

Note that the case  $k_1 = k_2 = 1$  represents the classic elastic interaction between the body and a particle. A similar model, in the three-dimensional setting, was considered in [27] by WEIDMAN and HERCZYNSKI. They studied rotating convex bodies like a ball, a cylinder and a parallelepiped of polygonal section in the particular case  $k_2 = 1$  with a specific tangential friction, and calculated only the force (and not its moment).

We shall adopt the following notation:

$M$	mass of the disc,
$r$	its radius,
$I$	its moment of inertia,
$\mu = I/Mr^2$	relative moment of inertia,
$v$	disc velocity,
$u =  v $	
$\omega$	angular velocity,
$\lambda = r\omega/u$	relative angular velocity,
$\rho$	density of the medium.

Additionally to the system  $\tilde{O}\tilde{x}_1\tilde{x}_2$  we consider the reference system  $Ox_1x_2$  moving together with the disc, where  $O$  is the disc center and the axis  $Ox_1$  points to the direction of its translation. Note that the system  $\tilde{O}\tilde{x}_1\tilde{x}_2$  from Fig. 2 coincides with that in Fig. 1. The disc rotates around  $O$  with the angular velocity  $\omega$ . Here and in what follows, the angular velocity and angles are measured counterclockwise. In this reference system, there is the rarefied flow of velocity  $-v = (-u; 0)^T$ . In fact both the systems  $Ox_1x_2$  and  $\tilde{O}\tilde{x}_1\tilde{x}_2$  are not

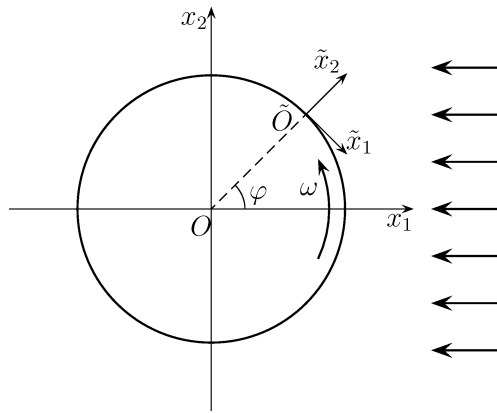


FIG. 2. Spinning disc in a rarefied flow.

inertial, however we will consider them as inertial ones due to the mentioned above Remark 1.

Suppose the velocity of a particle hitting the disc at the point  $\tilde{O}$  is written as  $\tilde{v} = (\tilde{v}_1; \tilde{v}_2)^T$  in the former reference system, and  $v = (v_1; v_2)^T$ , in the latter one. Then the formulas of instantaneous change of variables are as follows:

$$\begin{bmatrix} v_1 \\ v_2 \end{bmatrix} = \begin{bmatrix} \sin \varphi & \cos \varphi \\ -\cos \varphi & \sin \varphi \end{bmatrix} \begin{bmatrix} \tilde{v}_1 \\ \tilde{v}_2 \end{bmatrix} + r\omega \begin{bmatrix} -\sin \varphi \\ \cos \varphi \end{bmatrix},$$

$$\begin{bmatrix} \tilde{v}_1 \\ \tilde{v}_2 \end{bmatrix} = \begin{bmatrix} \sin \varphi & -\cos \varphi \\ \cos \varphi & \sin \varphi \end{bmatrix} \begin{bmatrix} v_1 \\ v_2 \end{bmatrix} + r\omega \begin{bmatrix} 1 \\ 0 \end{bmatrix},$$

where at the given instant the radius vector  $O\tilde{O}$  forms the angle  $\varphi$  with  $Ox$ .

Substituting  $v = (0; -u)^T$ , the velocity of a flow particle incident on the disc, in the former reference system one gets  $\tilde{v} = (r\omega - u \sin \varphi; -u \cos \varphi)^T$ . The velocity of the reflected particle computes as  $\tilde{v}^+ = (k_1(r\omega - u \sin \varphi); k_2 u \cos \varphi)^T$ . Making the reverse change of variables, one arrives at

$$v - v^+ = ((1 - k_1)r\omega + (k_1 + k_2)u \sin \varphi) \begin{bmatrix} \sin \varphi \\ -\cos \varphi \end{bmatrix} - (1 + k_2) \begin{bmatrix} u \\ 0 \end{bmatrix}.$$

Further, the angular momentum per unit mass transmitted by the particles at each boundary point

$$\Omega = -r(1 - k_1)(r\omega - u \sin \varphi).$$

The force (which is usually called force of resistance) and the moment of the force are obtained by integrating both  $v - v^+$  and  $\Omega$  over the part of the surface

involved in the interaction, that is,

$$(2.2) \quad R = ru\rho \int_{-\pi/2}^{\pi/2} (v - v^+) \cos \varphi \, d\varphi = -ru\rho (u\kappa_1 e_1 + r\omega\kappa_3 e_2),$$

$$(2.3) \quad R_I = -r^2 u \rho \int_{-\pi/2}^{\pi/2} (1 - k_1)(r\omega - u \sin \varphi) \cos \varphi \, d\varphi = -r^3 \omega u \rho \kappa_2,$$

where  $e_1 = (1; 0)^T$  and  $e_2 = (0; 1)^T$ .

Here we have introduced the new notation:

$$(2.4) \quad \kappa_1 = 2 - 2 \int_0^{\pi/2} k_1(\varphi) \sin^2 \varphi \cos \varphi \, d\varphi + 2 \int_0^{\pi/2} k_2(\varphi) \cos^3 \varphi \, d\varphi,$$

$$(2.5) \quad \kappa_2 = 2 - 2 \int_0^{\pi/2} k_1(\varphi) \cos \varphi \, d\varphi$$

and

$$(2.6) \quad \kappa_3 = \pi/2 - 2 \int_0^{\pi/2} k_1(\varphi) \cos^2 \varphi \, d\varphi.$$

These coefficients are dimensionless and reflect corresponding modes of interaction between the body and the particles. Namely, the coefficient  $\kappa_1$  is responsible for slowing down the disc, the coefficient  $\kappa_2$ , for its revolution slowing down, and  $\kappa_3$ , for deflection of the trajectory. Thus,  $\kappa_1$ ,  $\kappa_3$  and  $\kappa_2$  can be identified as generalised drag, lift and spin decay coefficients, respectively.

For example, the parameter  $\kappa_1$ , and therefore the drag force, is minimal when  $k_1 = 1$  and  $k_2 = 0$  and maximal for  $k_1 = 0$  and  $k_2 = 1$ . It is interesting to note that the friction parameter  $k_2(\varphi)$  does not influence the generalised coefficients  $\kappa_2$  and  $\kappa_3$ .

REMARK 2. In case when the parameter  $k_1$  takes its maximal value ( $k_1 = 1$ ), that corresponds to perfectly slippery disc boundary, the moment transmitted to the disc by a particle is directed toward the disc centre. No wonder that in this particular case the drag is parallel to the disc velocity and the moment of the force equals 0, while  $R = -ru^2 \rho \kappa_1 e_1$  and  $R_I = 0$ . Therefore the disc moves along a straight line with the angular velocity being constant. If, additionally,  $k_2 = 1$ , that is, in the case of perfectly elastic collisions, the force  $R = -\frac{8}{3} r \rho u^2 \cdot e_1$

equals two thirds of the corresponding force for the circumscribed square with the sides parallel and perpendicular to the direction of motion. Since the case of perfectly slippery boundary,  $k_1 = 1$ , is trivial in the sense of the disc dynamics, it is excluded from the further consideration.

As we will see later, the specific kind of asymptotic behaviour of the system (circumference, curve converging to a straight line, or converging spiral) is determined by the two parameters  $\varkappa_1$  and  $\varkappa_2$ , as well as by the relative moment of inertia  $\mu$ , whereas the parameter  $\varkappa_3$  determines quantitative properties of the special kind of trajectory. One can easily see that

$$4/3 < \varkappa_1 \leq 10/3, \quad 0 < \varkappa_2 \leq 2, \quad 0 < \varkappa_3 \leq \pi/2.$$

Moreover, the following inequality can be easily proven:

$$(2.7) \quad \varkappa_1 \geq \varkappa_2.$$

Indeed, from (2.4) and (2.5), it immediately follows

$$\varkappa_1 \geq 2 - 2 \int_0^{\pi/2} k_1(\varphi) \cos \varphi \sin^2 \varphi d\varphi \geq 2 - 2 \int_0^{\pi/2} k_1(\varphi) \cos \varphi d\varphi = \varkappa_2.$$

Let us determine the complete set of admissible values  $(\varkappa_1, \varkappa_2)$ . We have already seen that all values  $(\varkappa_1, \varkappa_2)$  belong to the rectangle  $[0, 2] \times [4/3, 10/3]$  and are situated above the line  $\varkappa_1 = \varkappa_2$ ; therefore the set is contained in the polygon  $ABFDE$  shown on Fig. 3a.

Note also that in the particular case when the coefficients  $k_1$  and  $k_2$  are constants, the following formulae hold true

$$(2.8) \quad \varkappa_1 = \frac{2}{3}(3 - k_1 + 2k_2), \quad \varkappa_2 = 2(1 - k_1), \quad \varkappa_3 = \frac{\pi}{2}(1 - k_1).$$

The first two relations establish a one-to-one correspondence between the space of constant parameters  $(k_1, k_2)$  (the square  $ABCD$  on Fig. 3b) and the parallelogram  $ABCD$  on Fig. 3a. This implies that the set of admissible parameters contains this parallelogram.

The following proposition shows that the space of admissible  $(\varkappa_1, \varkappa_2)$  depicted on the Fig. 3a is bounded by the segments  $AB$ ,  $CD$  and the curves  $AD$ :  $\varkappa_1 = g_{\min}(\varkappa_2)$  and  $BC$ :  $\varkappa_1 = g_{\max}(\varkappa_2)$ .

PROPOSITION 1. *The minimal and maximal values*

$$(2.9) \quad g_{\min}(x) = \inf\{\varkappa_1 : \varkappa_2 = x\} = 4/3 + x^3/12,$$

and

$$(2.10) \quad g_{\max}(x) = \sup\{\varkappa_1 : \varkappa_2 = x\} = 10/3 - (2 - x)^3/12,$$

are attained at the functions

$$(2.11) \quad k_1^*(\varphi) = \begin{cases} 1, & \text{if } \varphi \geq \arcsin(\varkappa_2/2), \\ 0 & \text{otherwise,} \end{cases} \quad k_2^*(\varphi) \equiv 0,$$

and

$$(2.12) \quad \tilde{k}_1(\varphi) = \begin{cases} 1 & \text{if } \varphi \leq \arcsin(1 - \varkappa_2/2), \\ 0 & \text{otherwise,} \end{cases} \quad \tilde{k}_2(\varphi) \equiv 1,$$

respectively. All the intermediate values between  $g_{\min}(x)$  and  $g_{\max}(x)$  are obtained by varying (continuously in  $L^1$ ) the functions  $k_1$  and  $k_2$  between their minimising (2.11) and maximising (2.12) values.

**P r o o f.** Here we prove that the infimum of

$$\varkappa_1(k_1, k_2) = 2 - 2 \int_0^{\pi/2} k_1(\varphi) \sin^2 \varphi \cos \varphi \, d\varphi + 2 \int_0^{\pi/2} k_2(\varphi) \cos^3 \varphi \, d\varphi,$$

under the condition

$$(2.13) \quad 2 - 2 \int_0^{\pi/2} k_1(\varphi) \cos \varphi \, d\varphi = x,$$

is attained at  $k_1 = k_1^*$ ,  $k_2 = k_2^*$ .

Make the change of variable  $z = \sin \varphi$  and denote  $f(z) = k_1(\arcsin z)$ . Then the condition (2.13) takes the form

$$\int_0^1 f(z) \, dz = 1 - x/2.$$

The function  $f^*(z) = k_1^*(\arcsin z)$  is obviously given by  $f^*(z) = 1$  if  $z \geq x/2$  and  $f^*(z) = 0$  otherwise.

One has

$$(2.14) \quad \varkappa_1(k_1, k_2) - \varkappa_1(k_1^*, k_2^*) \geq \int_0^1 (f^*(z) - f(z)) z^2 \, dz.$$

Denote by  $\Phi(z)$  the primitive of  $f^*(z) - f(z)$  such that  $\Phi(0) = 0$ , then  $\Phi(1) = \int_0^1 f^*(z) \, dz - \int_0^1 f(z) \, dz = 0$ . Moreover, the inequality  $\Phi(z) \leq 0$  holds for all  $0 \leq z \leq 1$ . Indeed, if  $z \leq x/2$ , one has  $\Phi(z) = -\int_0^z f(z) \, dz \leq 0$ , otherwise

$\Phi(z) = -\int_z^1 (1-f(z)) dz \leq 0$ . Thus, the right-hand side of (2.14) equals

$$\int_0^1 \Phi'(z) z^2 dz = -\int_0^1 \Phi(z) 2z dz \geq 0,$$

that finishes the proof. Finally, one readily calculates that  $\varkappa_1(k_1^*, k_2^*) = 8/3 + x^3/12$ .

To prove the second statement on supremum of Proposition 1, one can use the same line of reasoning as above.

Now, it remains to check whether all points are lying between the aforementioned limiting cases on the diagram from Fig. 3a. Indeed, consider the characteristic function of an interval  $[\varphi_1, \varphi_2]$ ,  $k_1(\varphi)$ , satisfying the condition (2.13), and choose  $k_2(\varphi) = k_2$  to be constant. By changing the parameters  $\varphi_1$ ,  $\varphi_2$  and  $k_2$  continuously from  $k_1^*$ ,  $k_2^*$ , 0 to  $\tilde{k}_1$ ,  $\tilde{k}_2$ , 1, one can observe that the value  $\varkappa_1(k_1, k_2)$  runs all the points of the interval  $[g_{\min}(x), g_{\max}(x)]$ .  $\square$

Recall that the set of values  $(\varkappa_1, \varkappa_2)$  corresponding to *constant* values of  $k_1, k_2$ , is the parallelepiped  $ABCD$  on Fig. 3a.

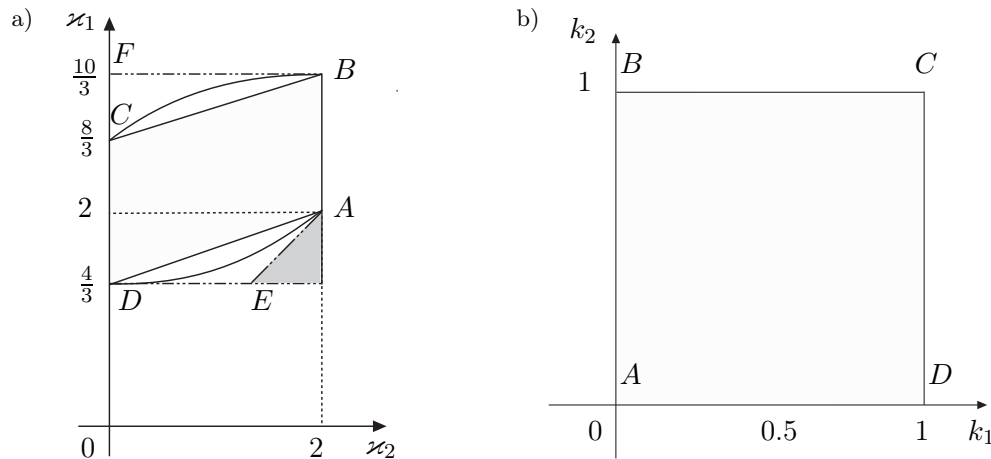


FIG. 3. The admissible spaces of auxiliary parameters  $\varkappa_2, \varkappa_1$  (Fig. 3a) and constant friction parameters  $k_1, k_2$  (Fig. 3b). The curves  $AD$  and  $BC$  are given (see (2.9), (2.10)) by the equations  $\varkappa_1 = g_{\min}(\varkappa_2)$  and  $\varkappa_1 = g_{\max}(\varkappa_2)$ , respectively. The curve  $AD$  is convex and touches the lines  $DE$  and  $AE: \varkappa_1 = \varkappa_2$  at the points  $D$  and  $A$ . The curve  $BC$  is concave and touches the line  $BF$  at the point  $B$ . The space of parameters  $\varkappa_1, \varkappa_2$  corresponding to constant values  $k_1$  and  $k_2$  is the parallelepiped  $ABCD$  on Fig. 3a.

REMARK 3. From (2.2) one can see that the transverse component of the force  $R$  equals  $R_T = -r^2 u \rho \omega \varkappa_3 e_2$  and thus is opposite to the instant rotation velocity of the disc front point,  $\omega r e_2$ , and therefore the *inverse* Magnus effect is

observed. Moreover, denoting by  $m$  the total mass of gas particles displaced by the disc,  $m = \pi r^2 \rho$ , the absolute value of this component can be written in the form (1.1) with the Maxwellian accommodation coefficient

$$\alpha = \frac{2}{\pi} \varkappa_3 = 1 - \frac{4}{\pi} \int_0^{\pi/2} k_1(\varphi) \cos^2 \varphi d\varphi.$$

In the case of constant  $k_1$  one gets  $\alpha = 1 - k_1$ .

REMARK 4. Although constant friction coefficients look at first glance like a natural choice, the opposite case is, in fact, more realistic. Thus any diffusion interaction leads to such relationships, if one will rewrite results from e.g. [28]. Moreover, as it has been discussed in [29, 30], at “grazing” angles of incidence,  $\varphi \approx 90^\circ$ , the specular reflection significantly raises. The simplest model for such an interaction can be written in the following quasi-linear form

$$\tilde{v}_1^+ = (k_1^0 \tilde{v}_1 - k_{12} \operatorname{sgn} \tilde{v}_1 |\tilde{v}_2|)_+, \quad \tilde{v}_2^+ = k_2 \tilde{v}_2,$$

where  $k_1^0$ ,  $k_{12}$  and  $k_2$  are constants. Rewriting these equations in the form (2.1), we get

$$k_1(\varphi) = k_1^0 (1 - f |\cot \varphi|)_+, \quad k_2 = \operatorname{const},$$

where  $f = k_{12}/k_1^0 > 0$ . Note that the same relationship could be obtained from the contact mechanics point of view where  $f$  is the Newton friction coefficient.

Then formulae (2.4)–(2.6) can be computed to give:

$$\begin{aligned} \varkappa_1(f) &= 2 + \frac{4}{3} k_2 - \frac{2}{3} k_1^0 \left( 1 - \frac{f}{\sqrt{f^2 + 1}} \right), \\ \varkappa_2(f) &= 2 - 2k_1^0 \left( 1 + f \ln \left( \frac{f}{\sqrt{f^2 + 1} + 1} \right) \right), \\ \varkappa_3(f) &= \frac{\pi}{2} - k_1^0 \left( \arctan \frac{1}{f} + 2f \ln \frac{f}{\sqrt{f^2 + 1}} \right). \end{aligned}$$

Note that the law (2.1) nonuniformly converges to the case  $k_1 = \operatorname{const}$  if  $f \rightarrow 0$ , while the other limiting case  $f \rightarrow \infty$  leads to  $k_1 = 0$ . One can easily obtain (2.8) passing to limit  $f \rightarrow 0$ , and  $\varkappa_1(\infty) = \frac{2}{3}(3 + 2k_2)$ ,  $\varkappa_2(\infty) = 2$ , and  $\varkappa_3(\infty) = \pi/2$  in the other case, that coincides with the expectations.

Let us investigate now an impact of the generalised friction coefficients discussed above on possible disc trajectory in the rarefied medium. We will need the following dimensionless parameters: the relative angular velocity,  $\lambda$ , and the relative moment of inertia,  $\mu$ , defined as follows

$$(2.15) \quad \lambda = r\omega/u, \quad \mu = I/(Mr^2).$$

One always has  $0 < \mu \leq 1$ ; if the mass is concentrated on the disc boundary (like in a football) then  $\mu = 1$ , if the mass is uniformly distributed over the disc (like in a golf ball) then  $\mu = 1/2$ , and if the mass is concentrated near the centre of the disc then  $\mu \ll 1$ .

It is convenient to introduce a complex velocity (corresponding to the initial coordinate system related to the particles). Namely, let us define  $v = ue^{i\theta}$ ; then the first coordinate vector in the system  $Ox_1x_2$  from Fig. 2 takes the form  $\epsilon_1 = e^{i\theta}$ , whereas the second one  $\epsilon_2 = i\epsilon_1$ . Moreover,  $u\epsilon_2 = iv$  and  $u = u(t)$  and  $\theta = \theta(t)$  depend on time. Recall here that  $u = |v|$ . In the complex notation, (2.2) and (2.3) can be written down as

$$R = -\rho ru(\varkappa_1 + i\lambda\varkappa_3)v, \quad R_I = -\rho r^2 u^2 \lambda \varkappa_2,$$

so the equations of disc dynamics

$$M \frac{dv}{dt} = R, \quad I \frac{d\omega}{dt} = R_I,$$

can be rewritten in the following form

$$M \left( \frac{d}{dt} u + iu \frac{d}{dt} \theta \right) = \rho r u^2 (-\varkappa_1 - i\varkappa_3 \lambda),$$

$$\mu M \frac{d}{dt} (\lambda u) = -\rho r u^2 \varkappa_2 \lambda.$$

In terms of new dimensionless variable  $\tau$  defined by  $d\tau = (\rho ru/M)dt$ , one finally gets the following set of differential equations in real variables

$$(2.16) \quad \frac{du}{d\tau} = -\varkappa_1 u,$$

$$(2.17) \quad \frac{d\lambda}{d\tau} = (\varkappa_1 - \varkappa_2/\mu)\lambda,$$

$$(2.18) \quad \frac{d\theta}{d\tau} = -\varkappa_3 \lambda,$$

with the initial conditions:  $u(0) = u_0$ ,  $\lambda(0) = \lambda_0$ ,  $\theta(0) = \theta_0$ .

The first equation is trivially integrated to obtain

$$(2.19) \quad u = u_0 e^{-\varkappa_1 \tau},$$

and the distance passed by the disc is computed as

$$s = \int_0^t u dt = s_* \tau, \quad \text{where} \quad s_* = \frac{M}{\rho r}.$$

REMARK 5. The dimensionless variable  $\tau$  is, in fact, the normalised distance. Moreover, it is easy to see that the path length,  $s$ , depends on time as  $\ln t$  or more precisely

$$(2.20) \quad s(t) = \frac{s_*}{\varkappa_1} \ln \left( 1 + \frac{u_0 \varkappa_1}{s_*} t \right).$$

REMARK 6. Without solving the rest of the system, one can immediately conclude that for any  $\lambda_0 > 0$ ,  $\varkappa_2 > 0$  and for a sufficiently small value of the parameter  $\mu$ , solution to the equation (2.17),  $\lambda(t)$ , exponentially vanishes, which is consistent with the definition of this parameter (see (2.15)).

Referring to the last two equations (2.17) and (2.18), there are three different cases corresponding to the sign of  $\varkappa_1 - \varkappa_2/\mu$ , namely

I.  $\mu \varkappa_1 = \varkappa_2$ . Solving the equations (2.17)–(2.18), one gets  $\lambda = \lambda_0$  and  $\theta = \theta_0 - \varkappa_3 \lambda_0 \tau$ . Thus, the trajectory is a circumference of radius  $s_*/(\lambda_0 \varkappa_3)$ .

II.  $\mu \varkappa_1 < \varkappa_2$ . The solution is

$$\begin{aligned} \lambda &= \lambda_0 e^{-(\varkappa_2/\mu - \varkappa_1)\tau}, \\ \theta &= \theta_0 + \frac{\mu \varkappa_3}{\varkappa_2 - \mu \varkappa_1} \lambda_0 \left( e^{-(\varkappa_2/\mu - \varkappa_1)\tau} - 1 \right). \end{aligned}$$

The trajectory is a curve converging to a straight line.

III.  $\mu \varkappa_1 > \varkappa_2$ . The solution is formally the same as in the Case II,

$$\begin{aligned} \lambda &= \lambda_0 e^{(\varkappa_1 - \varkappa_2/\mu)\tau}, \\ \theta &= \theta_0 - \frac{\mu \varkappa_3}{\mu \varkappa_1 - \varkappa_2} \lambda_0 \left( e^{(\varkappa_1 - \varkappa_2/\mu)\tau} - 1 \right), \end{aligned}$$

but now the trajectory is a converging spiral.

Regardless of the three discussed cases, the angular velocity of the disc can be written in a uniform way as

$$\omega = \frac{\lambda_0 u_0}{r} e^{-\varkappa_2 \tau / \mu}.$$

Finally one can rewrite all the variables as functions of time,  $t$ , instead of the dimensionless normalised distance,  $\tau$ , by adopting relation (2.20). In particular,

$$\begin{aligned} u &= u_0 \left( 1 + \frac{u_0 \varkappa_1}{s_*} t \right)^{-1}, \\ \omega &= \frac{u_0 \lambda_0}{r} \left( 1 + \frac{u_0 \varkappa_1}{s_*} t \right)^{-\frac{\varkappa_2}{\mu \varkappa_1}}. \end{aligned}$$

$$\theta = \theta_0 - \frac{\mu\kappa_3\lambda_0}{\mu\kappa_1 - \kappa_2} \left( \left( 1 + \frac{u_0\kappa_1}{s_*} t \right)^{\frac{\mu\kappa_1 - \kappa_2}{\mu\kappa_1}} - 1 \right).$$

Note that  $\omega(t)/u(t)$  is constant in the Case I, whereas  $\omega(t)/u(t)$  vanishes as  $t \rightarrow +\infty$  in the Case II and goes to infinity in the Case III.

Let us remind the specific case  $k_1 = 1$  discussed earlier in Remark 2 and excluded from the analysis as a trivial case. Indeed, in this case according to (2.6)  $\kappa_3 = 0$  and, regardless of the three cases defined above, one immediately concludes from (2.18) that  $\theta = \theta_0$ , so any possible trajectory is a straight line.

The three aforementioned cases completely describe dynamics of the spinning disc in the medium of motionless particles. However, the answer to the question which type of movement appears in each specific situation will depend on the friction parameters. We discuss this with examples in the next sections.

### 3. Discussions and numerical examples

Let us consider the simplest case when both the friction coefficients  $k_1$  and  $k_2$  are constants. Then the aforementioned Case I is defined by the condition

$$(3.1) \quad (3 - \mu)k_1 + 2\mu k_2 = 3(1 - \mu),$$

and the Cases II and III are given by the inequalities  $(3 - \mu)k_1 + 2\mu k_2 < 3(1 - \mu)$  and  $(3 - \mu)k_1 + 2\mu k_2 > 3(1 - \mu)$ , respectively. The straight line (3.1) divides the parameter square  $0 \leq k_1 < 1$ ,  $0 \leq k_2 \leq 1$  into two parts,  $L(\mu)$  and  $S(\mu)$ . On Fig. 4b the respective lines are depicted by solid line (for the case  $\mu = 1/2$ ) and

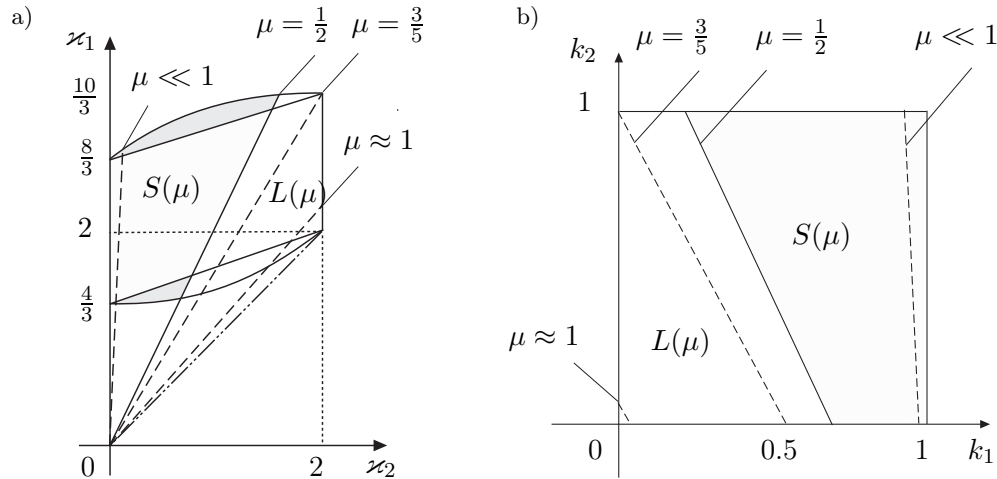


FIG. 4. Three possible cases of dynamical behaviour indicated in space of the auxiliary parameters  $\kappa_1$ ,  $\kappa_2$  (Fig. 4a) and the constant friction parameters  $k_1$ ,  $k_2$  (Fig. 4b)

dashed lines (for  $\mu = 3/5$  and two limiting cases  $\mu \approx 1$  and  $\mu \approx 0$ ). On the left part (L), the corresponding trajectory is asymptotically a straight line, and on the right part (S), it is a converging spiral. On the separation line, the trajectory is a circumference.

It is interesting to discuss influence of the inertia parameter  $\mu$  on the possible disc trajectory. For three specific values,  $\mu \approx 1$ ,  $\mu = 1/2$  and  $\mu \approx 0$ , we obtain the following statements:

(i) Let  $\mu = 1 - \varepsilon$  where  $\varepsilon \ll 1$  takes a small value. That corresponds to a all with mass concentrated near the boundary (football). Then for any couple  $(k_1, k_2)$  lying outside  $\varepsilon$ -neighbourhood of the origin of the parameter space (see Fig. 4b), the trajectory is always a converging spiral.

(ii) Let  $\mu = 1/2$  (golf ball). Then the separation line (3.1) takes the form  $5k_1 + 2k_2 = 3$ . This special case is depicted by solid line on Fig. 4b).

(iii) Let  $\mu = \varepsilon$  (the disc mass is concentrated near the centre). The separation line is located closely to the right vertical side of the square; so the trajectory is asymptotically straight for most parameters with couple  $(k_1, k_2)$  separated from the line  $k_1 = 1$ .

Finally, on Fig. 5, three cases of disc dynamics are provided for the particular values  $k_1 = 0.5$ ,  $k_2 = 0.25$ , (or, equivalently,  $\varkappa_1 = 2$ ,  $\varkappa_2 = 1$ ,  $\varkappa_3 \approx 0.753$ ),  $\lambda_0 = u_0 = 1$ ,  $s_* = 0.1$ . The cases  $L$ ,  $C$  and  $S$  are realised for different kinds of mass distribution inside the disc, characterised by the values  $\mu = 0.4$ ,  $0.5$  and  $0.6$ , respectively. In particular, the intermediate case of circumference ( $C$ ) is realised in the case of uniform mass distribution.

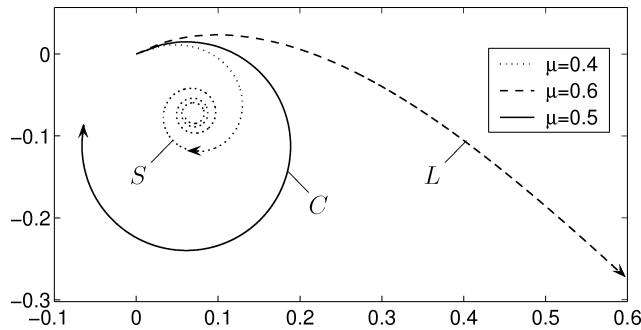


FIG. 5. Three cases of disc trajectory for  $\varkappa_1 = 2$ ,  $\varkappa_2 = 1$ : circumference ( $C$ ), asymptotic straight line ( $L$ ) and converging spiral ( $S$ ).

Summarizing the results presented in this paper, for any specific law of gas surface interaction (or, in other words, any friction regime) one can immediately conclude the trend of the body trajectory, knowing the inertial properties of the disc. Moreover, this enables to control the trajectory by varying the friction parameters and the moment of inertia.

## Acknowledgments

One of the authors (AP) was supported by *Centre for Research on Optimization and Control* (CEOC) from the “*Fundação para a Ciência e a Tecnologia*” (FCT), cofinanced by the European Community Fund FEDER/POCTI, and by FCT: research project PTDC/MAT/72840/2006.

The authors are grateful to the Reviewer for fruitful remarks.

## References

1. J. ASHENBERG, *On the effects of time-varying aerodynamical coefficients on satellite orbits*, *Acta Astronautica*, **38**, 75–86, 1996.
2. J. ASHENBERG, *Dynamical characteristics of a tethered stabilized satellite*, *J. Guid. Control Dyn.*, **20**, 1268–1271, 1997.
3. H.M. BARKLA, L.J. AUCHTERLONIE, *The Magnus or Robins effect on a rotating sphere*, *J. Fluid Mech.*, **47**, 437–447, 1971.
4. K.I. BORG, L.H. SÖDERHOLM, *Orbital effects of the Magnus force on a spinning spherical satellite in a rarefied atmosphere*, *Eur. J. Mech. B/Fluids*, **27**, 623–631, 2008.
5. K.I. BORG, L.H. SÖDERHOLM, H. ESSÉN, *Force on a spinning sphere moving in a rarefied gas*, *Physics of Fluids*, **15**, 736–741, 2003.
6. S.G. CHADWICK, S.J. HAAKE, *Methods to determine the aerodynamic forces acting on tennis balls in flight*, *Tennis Science and Technology*, S.J. HAAKE, A. COE [Eds.], *Proceedings of the 1st International Conference on Tennis Science and Technology*. Blackwell Science, Oxford, UK, pp. 127–134, 2000.
7. A.J. COOKE, *An overview of tennis ball aerodynamics*, *Sports Engineering*, **3**, 2, 123–129, 2000.
8. P.S. EPSTEIN, *On the resistance experienced by spheres in their motion through gases*, *Phys. Rev.*, **23**, 710–733, 1924.
9. S.G. IVANOV, A.M. YANSHIN, *Forces and moments acting on bodies rotating around a symmetry axis in a free molecular flow*, *Fluid Dyn.*, **15**, 449–453, 1980.
10. M.N. KOGAN, *Rarefied gas dynamics*, Plenum, New York 1969.
11. R.D. MEHTA, *Aerodynamics of sport balls*, *Annu. Rev. Fluid Mech*, **17**, 151–189, 1985.
12. R.D. MEHTA, J.M. PALLIS, *The Aerodynamics of a Tennis Ball*, *Sports Engineering*, **4**, 1–13, 2001.
13. P. MOORE, *The effect of aerodynamic lift on near-circular satellite orbits*, *Planet. Space Sci.*, **33**, 479–491, 1985.
14. I. NEWTON, *New theory of light and colours*, *Philosophical Transactions of the Royal Society London*, **1**, 678–688, 1672.
15. A.YU. PLAKHOV, T.V. TCHEMISOVA, *Force acting on a spinning rough disc in a flow of noninteracting particles*, *Doklady Math.*, **424**, 26–30, 2009.

16. L. PRANDTL, *Application of the "Magnus Effect" to the wind propulsion of ships*, Die Naturwissenschaft, **13**, 93–108; transl. NACA-TM-367, June 1926.
17. L. RAYLEIGH, *On the irregular flight of a tennis ball*, Messenger of Math., **7**, 14–16, 1877.
18. V.V. RIABOV, *The Magnus effect in rarefied gas near a spinning cylinder*, [in:] 15-th AIAA Applied Aerodynamics Conference, Atlanta, GA, June 23–25, 1997, Technical Papers, Pt. 2 (A97-31695 08-02).
19. V.V. RIABOV, *Numerical simulation of kinetic effects in low-density hypersonic aerodynamics*, [in:] Proceedings of the 25th International Congress of the Aeronautical Sciences, 3–8 September 2006, Hamburg, Germany.
20. B. ROBINS, *New principles of gunnery*, C. HUTTON, F. WINGRAVE [Eds.], London, 1805 (originally published in 1742).
21. S.I. RUBINOV, J.B. KELLER, *The transverse force on a spinning sphere moving in a viscous fluid*, J. Fluid Mech., **11**, 447–459, 1961.
22. S.A. SCHAAF, *Mechanics of rarefied gases*, [in:] Handbuch der Physik, Springer, Berlin, vol. VIII/2, 591–625 1963.
23. J.A. STORCH, *Aerodynamic disturbances on rapidly rotating spacecraft in free-molecular flow*, [in:] Proceedings of the 9th Biennial ASCE Aerospace Division International Conference on Engineering, Construction, and Operations in Challenging Environments, March 7–10, 2004, League City/Houston, TX, pp. 429-436.
24. G.A. TOKATY, *A history and philosophy of fluid mechanics*, Foulis, Henley on Thames 1971.
25. C.-T. WANG, *Free molecular flow over a rotating sphere*, AIAA J., **10**, 713, 1972.
26. R.G. WATTS, R. FERRER, *The lateral force on a spinning sphere: Aerodynamics of a curveball*, Am. J. Phys. **55**, 40–44, 1987.
27. P.D. WEIDMAN, A. HERCZYNSKI, *On the inverse Magnus effect in free molecular flow*, Physics of Fluids, **16**, L9–L12, 2004.
28. K. MOE, M.M. MOE, *Gas-surface interactions and satellite drag coefficients*, Planet. Space Sci., **53**, 793–801, 2005.
29. P.D. FIESELER, *A method for solar sailing in a low Earth orbit*, Acta Astronautica, **43**, 531–541, 1998.
30. E.D. KNECHTEL, W.C. PITTS, *Normal and tangential momentum accommodation for Earth satellite conditions*, Astronautica Acta, **18**, 3, 171–184, 1973.

Received March 3, 2009; revised version June 6, 2009.

---